Impact load estimation on retention structures with the discrete element method

7th International Conference on Debris-Flow Hazards Mitigation

Impact load estimation on retention structures with the discrete element method

Alessandro Leonardi[a,*], Ezio Calcagno[a], Marina Pirulli[a]

[a] *Politecnico di Torino, Corso Duca degli Abruzzi 24, 10121 Turin, Italy*

Abstract

The design of countermeasures such as barriers and filter dams needs an accurate estimation of the impact load. However, debris flows typically contain poorly sorted grains, whose size can span several orders of magnitude. Large grains can induce impulsive loads on a barrier, and potentially clog the openings designed to induce self-cleaning after an event. The current modeling techniques, mostly based on continuum-based depth-integrated approximations, cannot accurately describe these mechanisms, and analytical approaches often fail to tackle this complexity. In an effort to reproduce a realistic impact load, a sample flow composed of grains is reproduced with a three-dimensional model based on the Discrete Element Method (DEM). The mass impinges upon a barrier with a prescribed velocity. The barrier design is inspired by a monitored dam built on a catchment located in the Italian Alps, which features multiple outlets. The grains can clog the outlets, forming frictional arches. The load pattern on the barrier is analyzed in terms of single-grain impact and of collective behaviors. The impulse transferred by the granular mass to the structure is then used as input for a structural analysis of the barrier through a Finite Element analysis. The results highlight how frictional chains can induce loads that are substantially different from those determined by standard analytical approaches.

Keywords: Debris flow; Discrete element method, Flow-structure interaction; Hazard mitigation

1. Introduction

One of the methods to reduce risk associated with flow-like landslides is the construction of baffles (Law et al., 2015), deflectors (Ng et al., 2017b), or slit dams (Zhou et al., 2018). When installed immediately downstream from a catchment area, barriers are effective in breaking the energy of the flow early on, reducing its erosive power and effectively controlling the volume of large sediments transported. When sediments of different size are present, as is typical in debris flows, the barrier should retain the largest sediments (Piton and Recking, 2016). However, it is often preferable to avoid complete obstruction of the channel, in order to allow the regular flux of small sediments to occur in normal conditions. This is achieved by prescribing one or more outlets in the barrier (Marchelli et al., 2018a), whose size is designed as a function of the dimension of the minimum grain that should be retained.

A more rational evaluation of the impact force is a long-standing problem for the design of retention structures (Hungr and Jakob, 2015). The single cost of an experiment discourages the exploration of multiple geometries or conditions, and small-scale physical modeling suffers from scaling issues (Iverson, 2015). A cost-effective approach is to apply monitoring stations on existing barriers, in order to evaluate their performance, possibly both in vulnerability reduction and in robustness of the barrier design (Kwan et al., 2014).

The test case in exam is the sectional dam shown in Fig. 1(a), located in the municipality of St. Vincent, eastern Italian Alps. It consists of a concrete wall with multiple steel beams protruding from the top. Each beam has an IPE-type section (c), and is equipped with a strain gauge (a,c) to monitor the dam by recording the strain at the base of the steel beams. The dam is hit every summer from multiple stony debris flows, and is designed to retain the coarsest

* Corresponding author e-mail address*: alessandro.leonardi@polito.it*

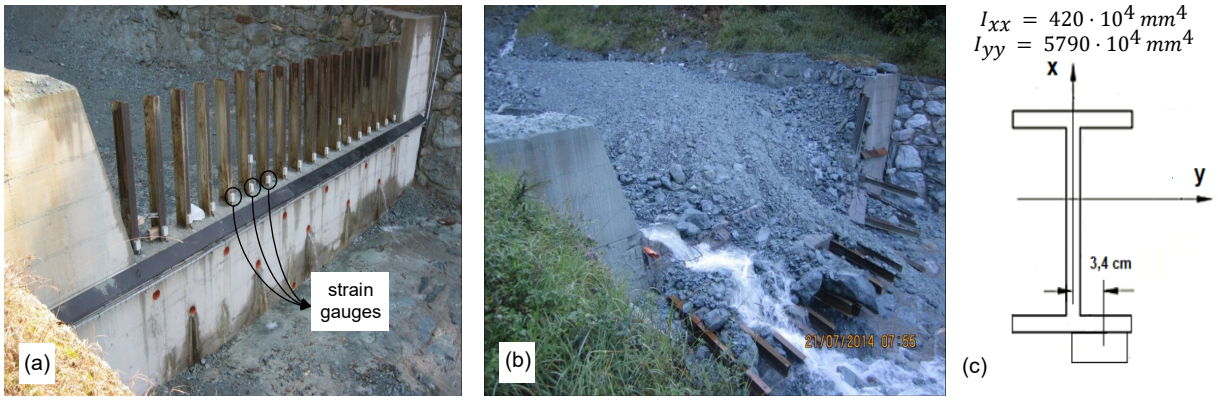

Fig 1. Illustration of the sectional dam used as study case, respectively before (a) and after (b) the collapse happened on 20/07/2014; (c) the cross section of the steel beams. The pictures are courtesy of Regione Autonoma Valle d'Aosta.

fraction of the grains. After every major event, the reservoir behind the dam is emptied in order to restore functionality. The dam dramatically collapsed during an event occurred in 2014, see Fig. 1(b). A discussion followed on the actual reason that induced the collapse. When activated by an impact, the sensors typically record compression (negative strain). However, it is not uncommon for sensors to record positive tension. This is puzzling, as it was originally believed that all sensors would only register compression when activated, since they are located on the side of the beam that does not face the flow.

In order to give an interpretation to the signals recorded on site, we use in this work the discrete element method (DEM). We evaluate the type of load exerted on the barrier, assuming the barrier itself is hit by a single surge of monodisperse grains. The output is plugged into a finite-element model (FEM) of the barrier as a time-history of external actions. A dynamic analysis is then performed, studying how the bending moments at the base of the beams evolve. The strain at the base is then compared to the site recordings.

2. Numerical model

The numerical procedure is outlined in Fig. 2(a). The debris flow is modelled with the DEM, which allows to obtain a time-history of load patterns on the barrier. The barrier itself is modelled as an elastic body with a FEM model, where the forces recorded in the DEM simulation are used as a set of external loads. This allows to compute the stress and strain fields on the barrier, and compare them to the data obtained from the monitored dam.

2.1. Discrete load model with DEM

We compute the load on the barrier using a simplified approach, where the debris flow is simulated as a collection of spherical particles of mean diameter $d_f = 0.2$ m. Moreover, the actual material composition is complex, including grains with different size and shape immersed in a liquid (Kaitna et al., 2016; Leonardi et al., 2018).

The debris flows recorded in St. Vincent are frequently multi-surge events. These surges can occur within minutes or separated by few hours. As a consequence, it is common that a second surge impacts the barrier before the first is removed. They impinge on the lowest portion of the barrier with a relatively high speed and belatedly on the upper portion, usually with a lower speed due to the barrier having already reduced the momentum of the flow at that point. In the DEM model, we simplify this scenario by considering only the upper half of the barrier, i.e. only the metal bars plus a portion of the concrete dam, for a total height of $h = 2.5$ m. We simulate only a total width of $w = 3i$, where $i = 2.5d_f = 0.5$ m is the spacing between two beams. We further consider that the particles reach the upper portion of the barrier with a homogeneous speed (Calvetti et al., 2018), see the example of Fig. 2(b). In spite of these assumptions, the model is able to capture many relevant aspects of the problem, as will be apparent in the following chapters.

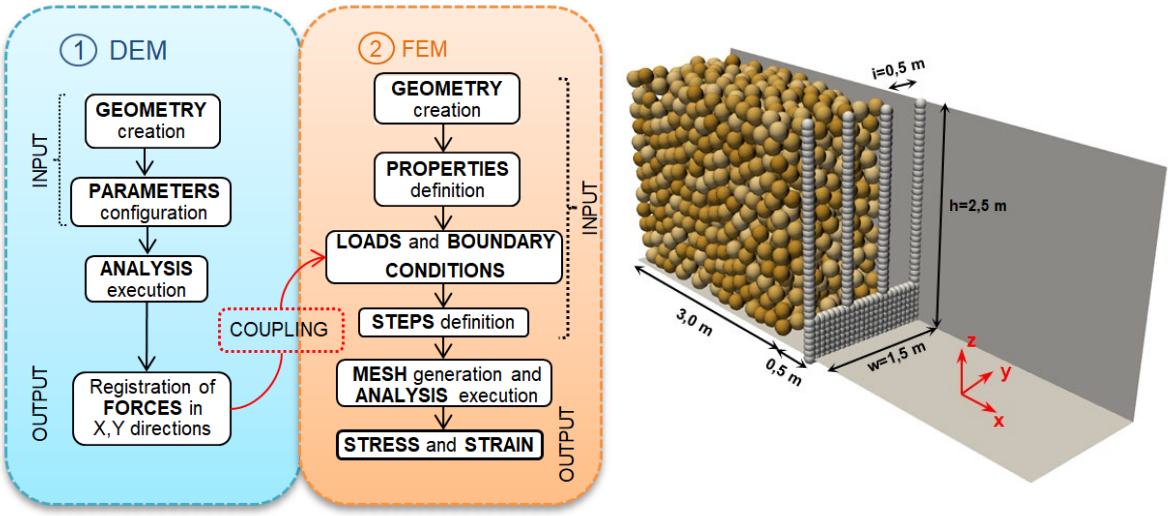

Fig. 2. (a) outline of the DEM-FEM model; (b) initial setup of the DEM simulation, with the discretization of the dam using spherical particles.

The DEM model employed for this study is implemented in the code by Leonardi et al. (2015; 2016). A Herzian contact model is used in the normal direction and the tangential contact model presented in Marchelli et al. (2018b) reproduces frictional effects. The numerical parameters used in this work are collected in Table 1. For their physical and numerical explanation, please refer to Marchelli et al. (2018b). The barrier is represented using an agglomeration of fixed spheres of constant diameter $d_b = 0.135$ m, overlapping by $d_b/2$. This greatly simplifies the computation of contact forces, as the same algorithm managing contact dynamics between the grains can be used to track the interactions with the barrier too.

Table 1. Parameters for the DEM flow model

DEM parameters	Value
Density ρ [kg/m^3]	2630
Diameter d_f [m]	0.2
Young modulus E [Pa]	$1.2 \cdot 10^9$
Poisson ratio ν [-]	0.2
Restitution coefficient ξ [-]	0.8
Tangential damping coefficient α_t [-]	0.5
Friction coefficient μ_s [-]	0.6
Rolling coefficient μ_r [-]	0.07
Mean particle diameter d [m]	0.2

Each of the barrier spheres registers a time-history of forces transmitted by the flow. Three samples of typical records are shown in Fig.3. The force is initially transmitted by quick impulsive loads (type A, red), whose direction is mainly aligned with the channel longitudinal direction, x. However, the grain size is large enough to induce jamming at the outlets. Therefore, immediately after the dynamic phase has finished, the grains jam and the load reduces to the transmission of the grains self-weight. However, the formation of the deposit is not immediately stable, and multiple ruptures and reorganization of the grains are observed for a relatively long period of time. This progressive clogging of the barrier causes a type of load that is semi-permanent (type B, blue), with every contact between barrier and grains transmitting a portion of the deposit weight through a frictional arch. The arches transmit a load both in direction x and in direction y. Therefore, strong force components F_y are registered at this stage. The deposit instabilities cause oscillations of the load, and also additional sharp impulses. Finally, after jamming is complete, some sensors register a final stationary load in both direction, due to the attainment of a stable jamming configuration of the deposit (type C, green).

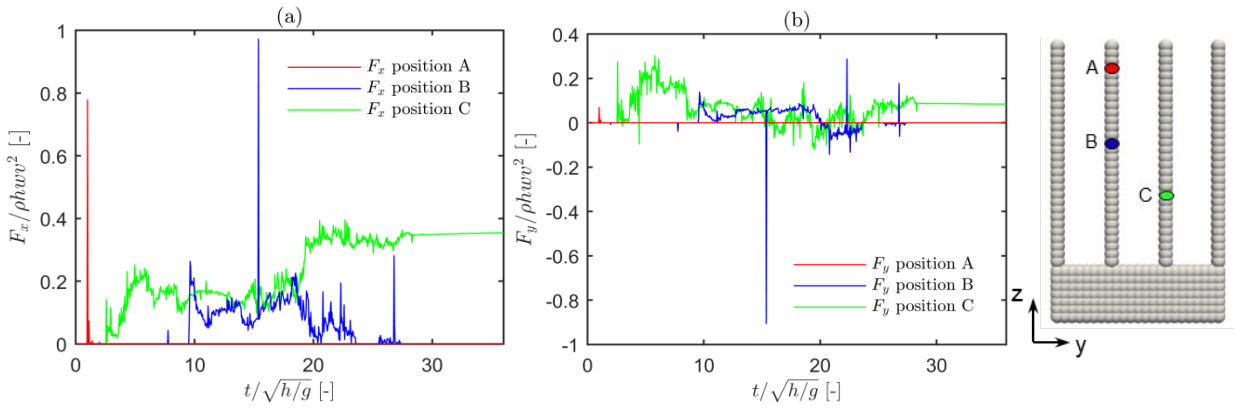

Fig. 3. Three sample loads registered at different locations on the barrier: (a) streamwise component F_x; (b) transversal component F_y.

2.2. Dynamic analysis of barrier response with a FEM model

The dynamic response of the barrier is obtained by assembling an FEM model (ABAQUS, www.3ds.com). The concrete basement is modelled using 3D brick elements, and the metal bars using 1D beams. The beams, as in the actual barrier, continue inside the basement for 1 m. Along this length, the beams lie embedded within the bricks, i.e. displacement of the beams is limited by the stiffness of the host material (Tabatabaei et al., 2014). Rotational degrees of freedom are instead simply constrained. The beams section is an IPE270, as in St.Vincent. The forces recorded with the DEM using the barrier sensors are given to the FEM model as point loads with a time-history of intensity. Therefore, 30 point loads are active for each beam. The concrete basement is modeled with fixed joint constraints on the base and edges. The material parameters are given in Table 2.

The stress-strain evolution over time is obtained through an explicit dynamic analysis with the central-difference rule. The system is overdamped, with damping factors set in order to reproduce the effects of the surrounding flow. During impact, the beams are surrounded by stony debris, which quickly dissipate the inertial load due to dynamic effects. Every 0.05 s the state of the system is saved for postprocessing.

Table 2. Parameters for the FEM model

FEM parameters	Value	
Materials	Concrete	Steel
Density ρ [kg/m^3]	2500	7850
Young modulus E [Pa]	$3.0 \cdot 10^{10}$	$2.1 \cdot 10^{11}$
Poisson ratio ν [-]	0.15	0.3
Damping factor α [-]	100.0	100.0
Damping factor β [-]	$1.0 \cdot 10^{-8}$	$1.0 \cdot 10^{-8}$

3. Reconstruction of the load patterns

Though the numerical workflow described in the previous section, the reaction in the barrier can be directly linked to specific stages of the interaction. Three instances are described in Fig. 4. In the first row, the stress field on the steel beams is reconstructed, and the beams themselves are depicted at the deformed state, with a displacement magnification of 2.5 ×. The second row shows the velocity of the particles close to the outlets, which allows to infer the dynamic state of debris mass at the same instant. Finally, the third row shows the in-plane component of the forces transmitted by the flow to the structure at that instant.

The beams have a much higher moment of inertia in direction x, see Fig. 1(c), and therefore exhibit reduced bending when loaded normally to the dam. The moment of inertial resisting bending in direction y is lower, therefore even a small in-plane force induces a significant bending, as can be observed at $t = 0.3$ s and $t = 19.0$ s. The first column in the figure corresponds to the dynamic impact (t=0.3s). At this instant jamming is not complete. There is a diffuse

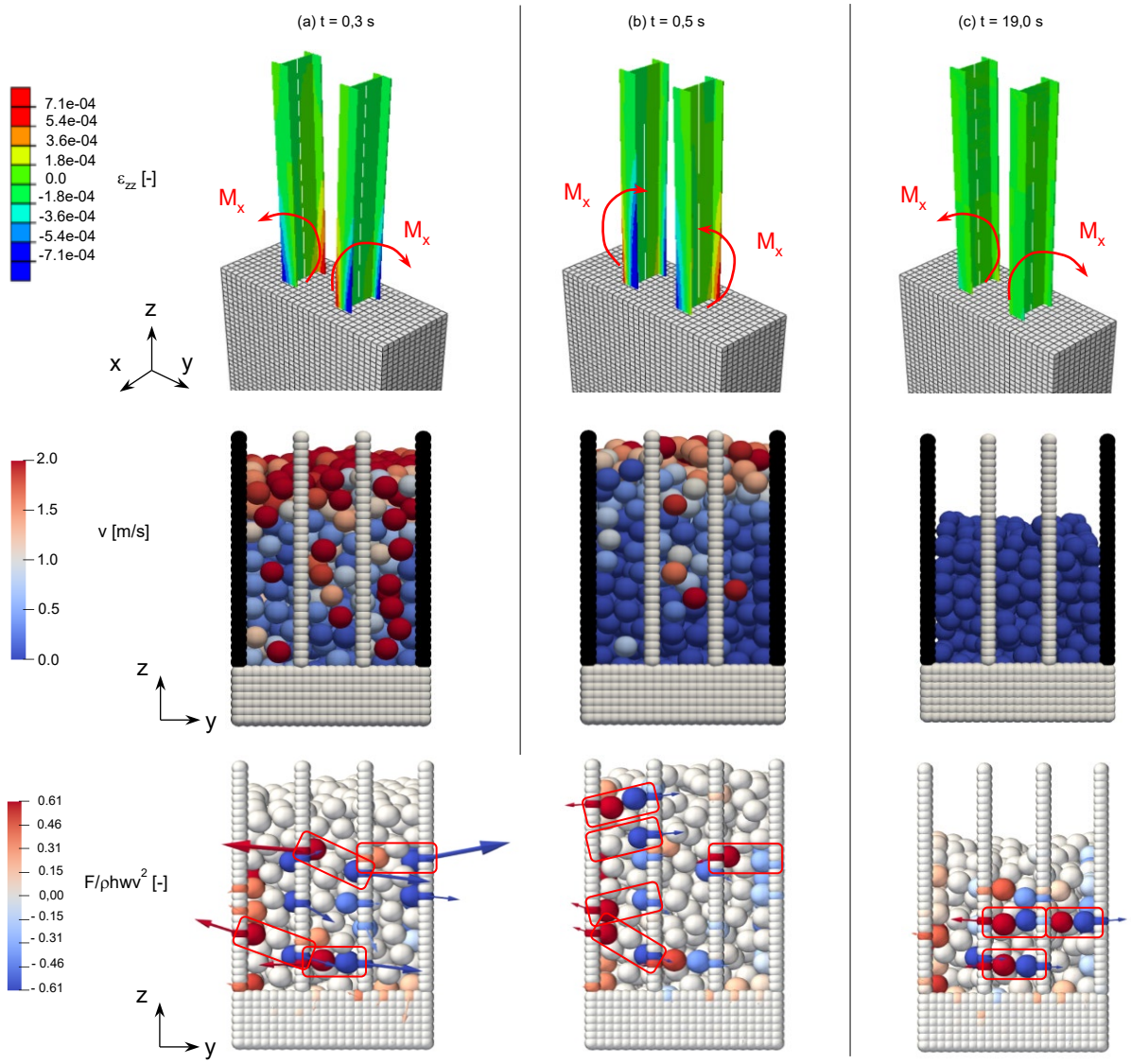

Fig. 4. Schematic of the mechanism of force transmission to be barrier, and corresponding strain field on the beams. A few granular arches are highlighted with red boxes.

outflow of material, but the central outlet already sees the formation of two granular arches that induce diverging loads on the beams (highlighted with red boxes in the figure). Therefore, the bending moments M_x at the base have opposite signs. Note that the bending moments M_y, conversely, are always positive.

On the second column is the interaction at $t = 0.5$ s. At that instant, jamming has completed and the lowest portion of the grains is not moving. The system is however not stable yet, and collapses are still occurring. Specifically, the figure shows that the central outlet is active, while the lateral ones are stable (Marchelli et al., 2018a). Consequently, the lateral outlets have more active arches than the central one (see the multiple red boxes in the figure), and exert a stronger in-plane load to the beams. This leads to a switch of the sign of M_x compared to the previous instant, which induces a converging deformation of the beams. The final, stationary configuration is shown at time $t = 19.0$ s on the third column. Here, the statistical process of particle rearrangement has terminated with strongest loads in the central outlet, overall similar to the one of the first column, and with diverging moments on the beams.

4. Interpretation of the strain signals measured on site

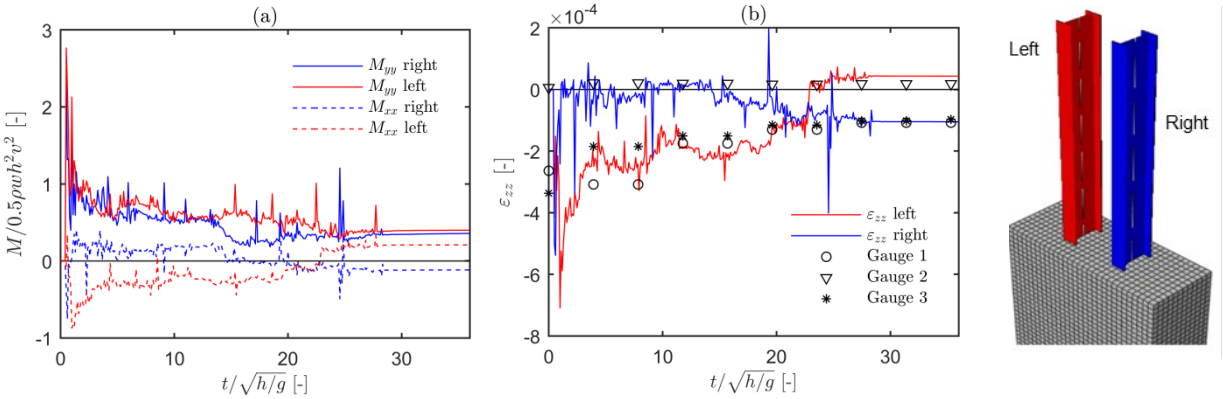

Fig. 5. Time-history of (a) the bending moment registered at the beam junction with the concrete basement, and (b) corresponding strains registered at the location where the strain gauges are installed.

The 3D nature of the barrier-flow interaction determines spurious stresses, which had not been accounted for in the barrier design. This observation provides an interpretation for the counterintuitive stresses recorded on the instrumented dam. Assuming the only actions are the bending moments on x and y, the strain at the instrument location can be estimated by using the simple formula for asymmetric bending

$$\varepsilon_{zz} = \frac{M_x}{I_x} d_x + \frac{M_y}{I_y} d_y, \qquad (1)$$

where (d_x, d_y) is the distance of the gauges from the section centers, see Fig. 1(c). The recorded moments are shown in Fig. 5(a). The moments in y are always positive and induce a compression (negative) strain. On the other hand, the moments in x do not have a preferential direction, and often switch from positive to negative and vice versa during the simulation. This corresponds to the statistical configuration of the in-plane loads due to the frictional arches, as shown with Fig. 4.

The bending moments in the two directions have the same order of magnitude, however the inertia moment in x is much smaller than the one in y. Therefore, the main factor that determines amplitude and sign of ε_{zz} is M_x, rather than M_y. This is confirmed by the FEM computations of ε_{zz}, shown in Fig. 5(b). The figure also shows three typical signals taken from the recording at St.Vincent. Notwithstanding the many simplifications adopted in the procedure, the model is able to capture the order of magnitude of the recorded strains. Moreover, it is able to explain the positive components registered by some sensors, e.g. Gauge 2 in Fig. 5(b).

5. Conclusions and outlook

We apply a numerical framework for the estimation of impact forces, and resulting reaction, exerted by a debris flow on a retention barrier. The framework employs the DEM for the simulation of the flow, and for recording the load pattern over the whole barrier. A FEM model processes the recorded load and perform a dynamic analysis of the structure response. The model describes how the flow interacts with the barrier though the formation and ruptures of frictional arches. This determines a type of load in the barrier that has a strong in-plane (transversal) component in addition to the more intuitive component orthogonal to the wall. The results are in excellent agreement with the type of signal recorded on site.

The analysis leads to two prescriptions for the design and monitoring of this type of barrier. Firstly, an effective monitoring system should be designed to give information at two locations on the same section, in order to infer the actual load from strain measurement. Most importantly, the stiffness of the structural element should always be prescribed as symmetrical, in order to cope with the in-plane component of the load. Assuming the load on the barrier to be orthogonal, as suggested by multiple codes and guidelines, might lead do grossly under designed barriers.

In this work, a simple one-way coupling has been implemented for the computation of forces. However, the large deformations of the beams probably alter the jamming mechanisms (Marchelli and De Biagi, 2018). To assess the feedback mechanism, a two-way coupling will be implemented in the future.

References

Calvetti, F., di Prisco, C. G., and Vairaktaris, E., 2015, Impact of dry granular masses on rigid barriers. IOP Conference Series: Earth and Environmental Science, v. 26, no. 1, 012036, doi: 10.1007/s11440-016-0434-z.

Hungr, O., and Jakob, M., 2005, Debris-flow Hazards and Related Phenomena, Springer-Verlag Berlin Heidelberg, doi: 10.1007/b138657.

Iverson, R. M., 2015, Scaling and design of landslide and debris-flow experiments: Geomorphology, v. 244, p. 9–20, doi: 10.1016/j.geomorph.2015.02.033.

Kaitna, R., Palucis, M. C., Yohannes, B., Hill, K. M., and Dietrich, W. E., 2016, Effects of coarse grain size distribution and fine particle content on pore fluid pressure and shear behavior in experimental debris flows: Journal of Geophysical Research: Earth Surface, v. 121, no. 2, p. 415–441, doi: 10.1002/2015JF003725.

Kwan, J. S. H., Chan, S. L., Cheuk, J. C. Y., and Koo, R. C. H., 2014, A case study on an open hillside landslide impacting on a flexible rockfall barrier at Jordan Valley, Hong Kong: Landslides, v. 11, no. 6, p. 1037-1050, doi: 10.1007/s10346-013-0461-x.

Law, P. R. H., Choi, C. E., and Ng, W. W. C., 2015, Discrete-element investigation of influence of granular debris flow baffles on rigid barrier impact: Canadian Geotechnical Journal, v. 7, p. 1–7, doi: 10.1139/cgj-2014-0394.

Leonardi, A., Cabrera, M., Wittel, F. K., Kaitna, R., Mendoza, M., Wu, W., and Herrmann, H. J., 2015, Granular-front formation in free-surface flow of concentrated suspensions: Physical Review E - Statistical, Nonlinear, and Soft Matter Physics, v. 92, no. 5, 052204, doi: 10.1103/PhysRevE.92.052204.

Leonardi, A., Wittel, F. K., Mendoza, M., Vetter, R., and Herrmann, H. J., 2016, Particle-Fluid-Structure Interaction for Debris Flow Impact on Flexible Barriers: Computer-Aided Civil and Infrastructure Engineering, v. 31, no. 5, p. 323–333, doi: 10.1111/mice.12165.

Leonardi, A., Pokrajac, D., Roman, F., Zanello, F., and Armenio, V., 2018, Surface and subsurface contributions to the build-up of forces on bed particles: Journal of Fluid Mechanics, v. 851, p. 558–572, doi: 10.1017/jfm.2018.522.

Marchelli, M., Leonardi, A., and Pirulli, M., 2018a, The clogging mechanism of debris-flow material in the multiple outlets of sectional barriers: Geoingegneria Ambientale e Mineraria, v. 153, no. 1, p. 78–85.

Marchelli, M., Leonardi, A., and Pirulli, M., 2018b, On the efficiency of slit dams in retaining granular flows: Géotechnique, doi: 10.1680/jgeot.18.p.044 (in press).

Marchelli, M., and De Biagi, V., 2018, Dynamic effects induced by the impact of debris flows on protection barriers: International Journal of Protective Structures, v. 10, no. 1, p. 1-12, doi: 10.1177/2041419618798378.

Ng, C. W. W., Choi, C. E., Goodwin, G. R., and Cheung, W. W., 2017, Interaction between dry granular flow and deflectors: Landslides, v. 14 no. 4, p. 1375–1387, doi: 10.1007/s10346-016-0794-3.

Pirulli, M., Barbero, M., Marchelli, M., and Scavia, C., 2017, The failure of the Stava Valley tailings dams (Northern Italy): numerical analysis of the flow dynamics and rheological properties: Geoenvironmental Disasters, v. 4, no. 1, p. 1-15, doi: 10.1186/s40677-016-0066-5.

Piton, G., and Recking, A., 2016, Design of Sediment Traps with Open Check Dams. I: Hydraulic and Deposition Processes: Journal of Hydraulic Engineering, v. 142, no. 2, 04015045, doi: 10.1061/(ASCE)HY.1943-7900.0001048.

Tabatabaei, S. A., Lomov, S. V., and Verpoest, I., 2014, Assessment of embedded element technique in meso-FE modelling of fibre reinforced composites: Composite Structures, v. 107, p. 436–446, doi: 10.1016/j.compstruct.2013.08.020.

Zhou, G. G. D., Hu, H. S., Song, D., Zhao, T., and Chen, X. Q., 2018, Experimental study on the regulation function of slit dam against debris flows: Landslides, v. 16, no. 1, p. 75-90, doi: 10.1007/s10346-018-1065-2.